Journal of
Computational and Theoretical Nanoscience
Vol. 14, 1–12, 2017

Prediction of Solar PV Panel Temperature Using Mathematical Models and Artificial Neural Networks

R. Vijaykumar[1,*], R. Rudramoorthy[2], and Ashish Mangalore Rao[3]

[1] *Robert Bosch Engineering and Business Solutions India Pvt. Ltd., Coimbatore, India*
[2] *PSG College of Technology, Coimbatore, India*
[3] *Robert Bosch Engineering and Business Solutions India Pvt. Ltd., Bangalore, India*

Increasing population and decreasing sources of conventional energy sources has resulted in decreased availability of energy per person. In this context, the role and relevance of solar energy has been increasing at a very rapid pace in the recent times. It is common knowledge that the output of a solar panel increases with irradiation. However increase in irradiation with ambient temperature increase also increases module temperature. In order to operate the solar panel at optimum efficiency, it is vital to monitor the rise in module temperature. This is because after a certain temperature, solar cells operate at decreased efficiencies due to negative thermal coefficient. This paper aims to compare and develop temperature prediction schemes for solar panels in the Indian environment and thus bring the error in prediction down in the range of 5–10% or less. The logged data for every second for a period of 12 days from 1st December 2013 to 12th December 2013, recorded at Adugodi, Bangalore, India is used as the primary reference for model development. A collection of mathematical models made by various researchers is tested for daily averages of data available for two different types of solar cells to test generality. Few well behaving models are shortlisted and tested for per second and five-minute average data. A workflow is developed and described for the same. The workflow gives a visual representation of the error, enabling the user to combine different models based on their regions of optimum operation. The concept of Artificial Neural Networks is applied and tested for its validity with the data in hand. The different schemes of prediction are then compared to pick the best one. The prediction schemes outlined in this paper give minimal error which is in the range of 3.5–5% for Neural Networks and less than 10% on an average for mathematical models.

Keywords: Solar Panels, Solar Radiation, Temperature Prediction, Artificial Neural Networks, MATLAB, Simulink, Mathematical Modeling.

RESEARCH ARTICLE

1. INTRODUCTION

Solar panel temperature is one of the important factors that affects how much electricity panels will produce. The more sunshine they get, the hotter the panels get and this in turns counteracts the benefit of the sun. The solar panel temperature affects the maximum power output directly. As solar panel temperature increases, its output current increases while the voltage output is reduced linearly. Since power is equal to voltage times current this property means that the warmer the solar panel the less power it can produce as can be seen in Figure 1. The power loss due to temperature is also dependent on the type of solar panel being used. In locations closer to the equator the problems of heat loss could become substantial over the full year and warrant looking at alternatives. This paper models the temperature rise in hotter conditions so as to make performance predictions more reliable.

The primary objective is to estimate the rise in solar panel internal module temperature for the c-Si type of panel within an error of 5–10% or less. In order to realize this, it is necessary to meet the following objectives in phases as outlined.

- Collect and Test Mathematical models for cell temperature for data sampled for longer time intervals
- Design a workflow and test well behaved mathematical models for data sampled for shorter time intervals
- Develop a neural network to improve accuracy of prediction and compare with the mathematical models.

*Author to whom correspondence should be addressed.

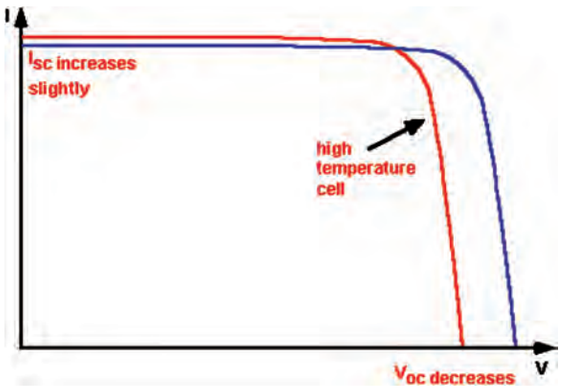

Fig. 1. Effect of temperature on panel performance.[1]

In short, by feeding various input parameters like wind speed, ambient temperature, irradiance, the output parameters expected is the module temperature.

By knowing the temperature of the solar panel beforehand, it is possible to develop schemes to lower the temperature as required or strategically locate the solar panels in windy areas where the air flowing over the panels plays the role of a natural coolant. By predicting temperatures at different parts of day, it is possible to operate the solar panels with maximum efficiency.

RESEARCH ARTICLE

2. METHODOLOGY

2.1. Literature Review

The transmissivity of the panel must be modelled appropriately. This was seen from Elnozahy et al.,[2] who have investigated effect of module temperature and dust on performance of the PV module by means of experimental studies on a series of modules grouped into 'standard modules' and 'continuous cooled and cleaned PV module. The results showed a decrease by 45.5% and 39% in module temperature measured at the front and rear faces respectively on the PV module as compared to standard modules with no cleaning and cooling.

Different models where selected for each step and their predictions where compared with data obtained by measurement similar to the methodology followed in Araneo et al.[3] They also highlighted the modelling of different subsystems of the PV system.

Ya'acob et al.[4] suggested development of an alternative model apart from the existing NOCT model called the t_{FOCT} model. This aims to model systems in tropical conditions and was found to have higher accuracy than the NOCT model in these conditions. The most frequent values of the parameters in tropical conditions which influence panel temperature were taken as the standards for the t_{FOCT} model. Further, Jakhrani et al.[5] discussed the different approaches to model solar cell modules namely steady state and non-steady state models. Different tests were conducted on existing models and one model was singled out as the most appropriate for their application. The models developed by JakhraniandYa'acob were considered and used for this project. Migan[6] discusses the prediction of panel temperature on the basis of irradiance and wind speed.

Further, methods to model encapsulation were discussed along with finding the effective irradiances. However, Muzathik[7] came up with a simple formula for predicting the panel temperature. A regression analysis was carried out for three input variables namely ambient temperature, wind speed and irradiance with panel temperature as the output variable which was an improvement from the method adopted in Ref. [8]. Thus an empirical formula was arrived at in this paper. These empirical formulae were used for mathematical model based temperature prediction in this project.

The various constant parameters are specified for the solar panels. Reference [10] specifies the parameters for the CIS panels while Ref. [9] specifies the parameters for the c-Si m panel.

Karatepe et al.[11] bought out a novel approach to model a solar cell output with ANN. The input parameters like radiation, cell temperature and wind speed were fed to derive the current, voltage output power and so on. A fairly accurate model was obtained. From this paper it was seen that neural networks could be applied in the context of cells.

The detrimental effects of high temperature were seen in El-Din et al., (2013).[12] They reported effect of ambient temperature on performance of different types of PV cells at different location in Egypt. For analysis of performance of PV module the average value was obtained through the results recorded for 5 trials with respect to all temperatures and solar irradiances. The presented graphs indicated that output voltage of the solar panel decreased with the increase in temperature and the output current (I_{sc}) slightly increased with temperature due to increase in R_{series} and R_{shunt}. The R_{series} increases voltage drop that lead to decrease in open circuit voltage (V_{OC}) as well as PV cell efficiency. Rahman et al.,[13] highlighted effect of temperature, irradiance and clearness index on performance of Solar PV module. The MATLAB/Simulink model was used to indicate that cell temperature rise lead to decrease in module power output due to fall in the open circuit voltage.

The equations representing the solar panel are explained by Swingshackla et al.[14] and Ciulla et al.[15] They provide an extensive coverage of the mathematical model of solar cells at various conditions of operations.

2.2. Description of Solar Panel Installation and Specifications

The site consists of three PV plant technologies each having an installed capacity of about 10 kW. All the modules are inclined at an angle of 15° facing south to allow natural

cooling effect and to avoid dust deposition to some extent. Two 3-phase transformers less inverters of each 10 kW are used for crystalline technologies and three 1-phase transformer based inverters of each 3.6 kW are used for thin film technologies.

The PV plant was installed and started working in the year 2010. The available power output and other meteorological parameters like wind speed, ambient temperature, module temperature, power output, solar irradiation and so on were recorded from 1st December 2013 to 12th December 2013 and these data were taken for study. The measurement unit is located at Adugodi, Bangalore. The panels at this location are mounted at an angle of 15 degrees. The PV system considered for this study has specific instruments to measure the input and output parameters. Two pyranometers each with an error of less than 10 W/m^2 have been used to measure the Global Horizontal Irradiance (GHI) and plane of array irradiance. An anemometer with a measurement range of 0.5 m/s to 50 m/s has been used to measure the wind speed at the plant site. Air temperature and module back panel temperature was measured using a calibrated thermocouple. The power output, solar radiation, air temperature, wind speed and module back panel temperature are recorded by a data logger. The measurement unit consists of two types of modules c-Si and CIS cell. The block diagram of the measuring system is as shown in the Figure 2.

A copper indium gallium selenide solar cell is a thin-film solar cell used to convert sunlight into electric power. It is manufactured by depositing a thin layer of copper, indium, gallium and selenide on glass or plastic backing, along with electrodes on the front and back to collect current. Because the material has a high absorption coefficient and strongly absorbs sunlight, a much thinner film is required than of other semiconductor materials.

The power generated at the CIS PV array end is 10.02 kW. The rated power of each module is 60 W.[10] As a result, 167 modules are used to get the required output power. The area of each module is 0.610236 m^2 and the total active area of the system is 101.9094 m^2. The CIS modules are arranged in the following manner as to get required power which is depicted in Figure 3.

4 strings/7 modules—4 sets
4 strings/7 modules—1 set
3 strings/9 modules—1 set.

Further another type of solar panel is explored. The cell used here for power generation is a conventional monocrystalline silicon cell.[9] The power generated at the c-Si PV array end is 10.34 kW. The rated power of each module is 235 W. As a result, 44 modules are used to get the required output power. The area of each module is 1.46016 m^2 and the total active area of the system is 64.24704 m^2. The c-Si modules are arranged in the following manner to get required power. 2 strings/22 modules—1 sets.

The arrangement of the c-Si PV array is as shown in Figure 4.

Mathematical models make use of different parameters mentioned in the specifications. In this section the meaning of the different parameters used are explained. STC refers to standard temperature conditions which is the conditions at which manufacturers test their panels and provide specifications. NOCT is the Nominal operating cell temperature conditions. These conditions are more practical than the STC conditions.

T_{NOCT} refers to the nominal operating cell temperature for which the panel is rated. From Refs. [9, 10] the T_{NOCT} for c-Si m60 and CIS cells are 48.40 °C and 46 °C respectively. T_{aNOCT} refers to the ambient nominal cell operating temperature which has been given as 20 °C in the

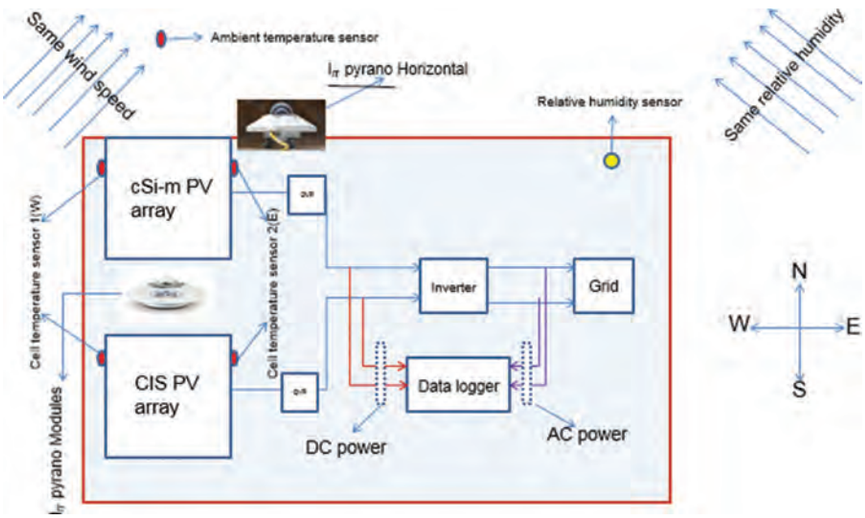

Fig. 2. Measuring arrangement of PV system.

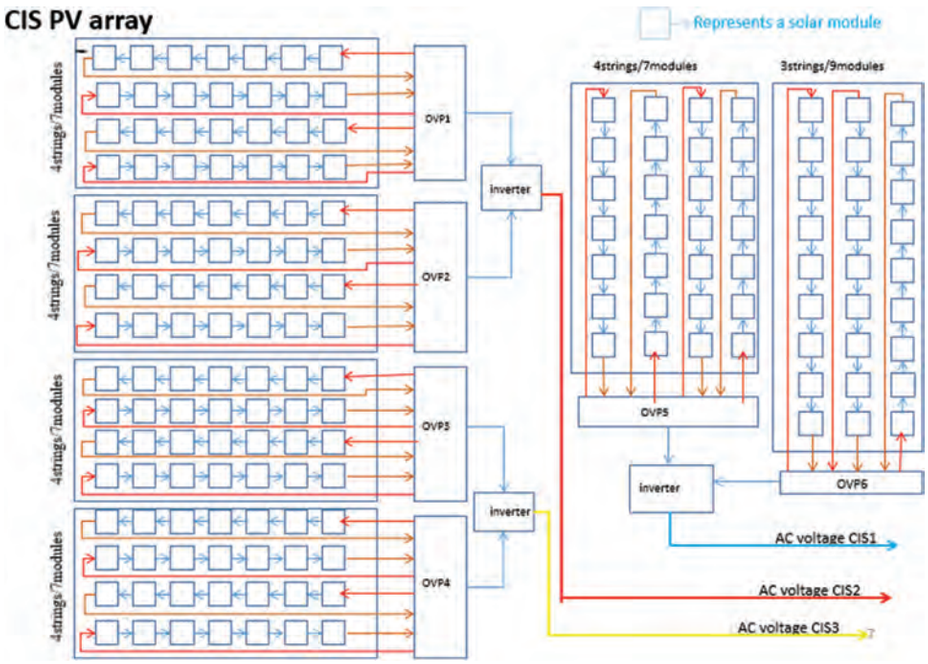

Fig. 3. Block diagram of CIS panel setup.

datasheets. G_{NOCT} refers to the irradiation at NOCT conditions which is about 800 W/m^2. β_{STC} gives the degradation factor of the panel per degree rise in temperature. Similarly, G_{STC} and T_{STC} correspond to irradiation and temperature at STC conditions. The areas of the panels are also known from the datasheets. All the required data for the c-Si and the CIS cells are tabulated in Table I given below.

We further need to calculate η_{STC} for both the panels. The equation to calculate η_{STC} is as shown below

$$\eta_{STC} = \frac{\text{Rated Power Output at STC}}{\text{Surface area} * G_{STC}} \quad (1)$$

For c-Si m60 panel,

$$\eta_{STC} = \frac{235}{1.6434 * 1000} = 0.1429$$

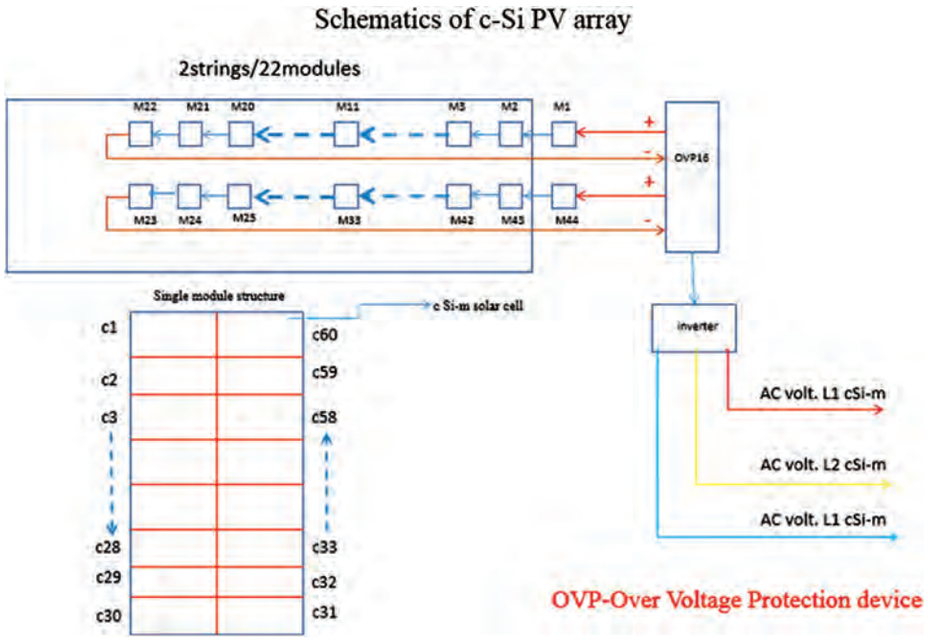

Fig. 4. Block diagram of c-Si panel setup.

Table I. The specifications of the solar cells.

c-Si m60		CIS panel	
T_{NOCT}	48.4 °C	T_{NOCT}	46 °C
T_{aNOCT}	20 °C	T_{aNOCT}	20 °C
G_{NOCT}	800 W/m^2	G_{NOCT}	800 W/m^2
β_{STC}	−0.47% W/°C	β_{STC}	−0.53% W/°C
T_{STC}	25 °C	T_{STC}	25 °C
Area of one panel	1.6434 m^2	Area of one panel	0.610236 m^2
Rated power output at STC	235 W	Rated power output at STC	60 W
G_{STC}	1000 W/m^2	G_{STC}	1000 W/m^2

For the CIS panel,

$$\eta_{STC} = \frac{60}{0.610236 * 1000} = 0.09843$$

It is also necessary to compute the transmissivity of the materials enclosing the solar cells and the absorptivity of the solar cells. It is found that transmissivity of glass $\tau_{glass} = 0.92$ and transmissivity of EVA film, $\tau_{EVA\,film} = 0.91$. This gives an effective transmissivity τ of 0.8372. Further, the absorptivity of the cell is taken to be about $\alpha = 0.96$. This gives us the effective value of $\tau \cdot \alpha \approx 0.8$. Thus, all the important parameter required for the purposes of mathematical modelling have been found.

3. TEMPERATURE PREDICTION WITH MATHEMATICAL MODELS

The main focus of the paper is to accurately predict the cell temperature of the c Si-m solar module. However, the same tests for validation are also carried out with the CIS panels. Similarity in the results ensures that the mathematical models have fairly diverse scope and are applicable to a wide variety of cell configurations. The different mathematical models used are as stated.[14–17] All the parameters and constants to be used in the models must be taken into account. The incident in plane irradiance is G and the ambient temperature is T_a. The local wind speed close to the module is given by v_w. In the formulae to follow, T_c is the cell temperature, T_{NOCT} is the cell temperature rated for Nominal Operating Cell Temperature (NOCT) conditions. T_{aNOCT} is the ambient temperature rated for NOCT conditions and G_{NOCT} the irradiance for NOCT conditions. Equations (2)–(15) bring out the various cell temperature models available in existing literature.

This is the simplest and most common model used to predict the temperature of the solar cell.[18] It makes use of only two variables namely the irradiance and the ambient temperature and it is given by the following equation:

$$T_c = T_a + G \cdot \frac{T_{NOCT} - T_{a,\,NOCT}}{G_{NOCT}} \quad (2)$$

The Kurtz model is mentioned in by Schwingshackl et al.[14] which is given by,

$$T_c = T_a + G \cdot e^{-3.473 - 0.0594 \cdot v_w} \quad (3)$$

The Koehl model is outlined in Ref. [15] which is given by,

$$T_c = T_a + \frac{G}{(U_0 + U_1 \cdot v_w)} \quad (4)$$

The values of U_0 and U_1 are constants specified by Koehl, which are given to be 30.02 and 6.28 respectively.

The Scoplaki model 2[25] makes use of the following equation,

$$T_c = T_a + \frac{G}{G_{NOCT}} \cdot (T_{NOCT} - T_{a,\,NOCT}) \cdot h_{wNOCT} \cdot \frac{[1 - n_{STC} \cdot ((1 - \beta_{STC} \cdot T_{STC})/(\tau \cdot \alpha))]}{h_w(v)} \quad (5)$$

Where h_w is the wind convection coefficient and is given by $h_w = 5.7 + 2.8.\ v_w$ for the Scoplaki 2 case and $h_{w,\,NOCT}$ is a constant value of 8.5.

The Mattei models[16] make use of the following base equation.

$$T_c = U_{PV}(v) \cdot T_a + G \cdot \frac{[\tau \cdot \alpha - n_{STC}(1 - \beta_{STC} \cdot T_{STC})]}{(U_{PV}(v) + \beta_{STC} \cdot n_{STC} \cdot G))} \quad (6)$$

Where, $U_{PV}(v_w) = 26.6 + 2.3 * v_w$ for the Mattei 1 model and $U_{PV}(v_w) = 24.1 + 2.9 * v_w$ for the Mattei 2 models.

The equation for the Homer Model as outlined in Ref. [17] is as follows,

$$T_c = \frac{T_a + (T_{cNOCT} - T_{a,\,NOCT})(G/G_{GNOCT})(1 - (n_{STC}(1 - \alpha T_{STC}))/(\tau\alpha))}{1 + (T_{cNOCT} - T_{a,\,NOCT})(G/G_{NOCT})((n_{STC}(\alpha T_{STC}))/(\tau\alpha))} \quad (7)$$

The Muzathik model is an empirical model based on regression analysis to input data. The input variables are the wind speed, the incident radiation and the ambient temperature.[15] The empirical relationship between them is as follows,

$$T_c = 0.943 \cdot T_a + 0.0195 \cdot G - 1.528 \cdot v_w + 4.3 \quad (8)$$

These equations are the ones stated by Rodolfo et al.[15] They are as follows Rodalfo-Umberto-Salvatore (RUS) 1 is as given by,

$$T_c = T_a + \frac{0.32}{8.91 + 2 \cdot v_w} \cdot G \quad (9)$$

The RUS-2 model is given by,

$$T_c = 0.943 \cdot T_a + 0.028 \cdot G - 1.528 \cdot v_w + 0.35 \quad (10)$$

And the RUS-3 model is given by,

$$T_c = T_a + (0.0138 \cdot G \cdot (1 + 0.031 \cdot T_a) \cdot (1 - 0.042 \cdot v_w) \quad (11)$$

RESEARCH ARTICLE

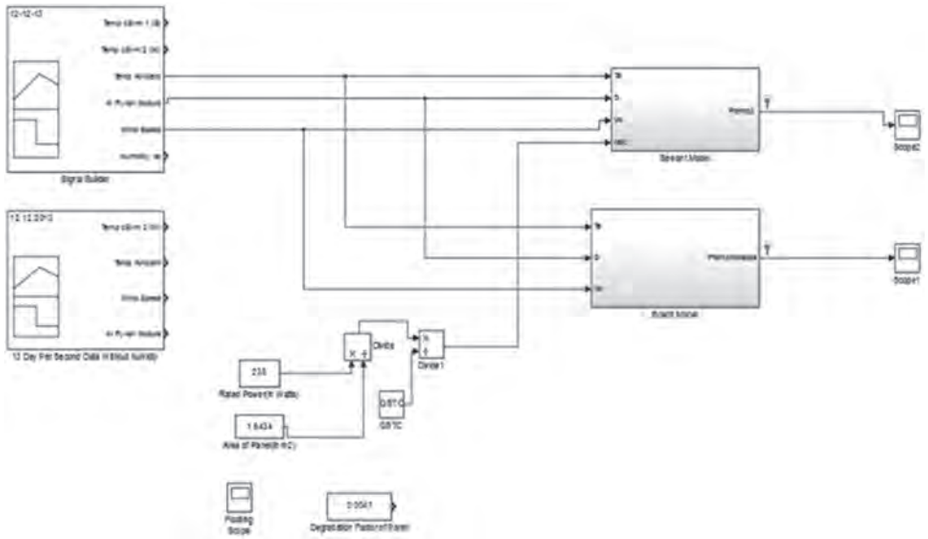

Fig. 5. Mathematical models in Simulink.

The McAdams model[14] is given by the following equation,

$$T_c = T_a + (G/G_{NOCT}) \cdot (9.5/(5.7 + 3.8 \cdot v_w)) \cdot (T_{NOCT} - T_{a,\,NOCT})\left(1 - \frac{n_{STC}}{0.9}\right) \quad (12)$$

The Servant Model[16] for temperature prediction is given by the following relation,

$$T_c = T_a + 0.0138 * G * (1 + 0.031 * T_a)(1 - 0.042 \cdot v_w) \cdot (1 - 1.0538 \cdot n_{STC}) \quad (13)$$

The King model follows the relation[14] given by,

$$T_c = T_a + \left(\frac{G}{G_{NOCT}}\right) \cdot (0.0712 \cdot v_w^2 - 2.411 \cdot v_w + 32.96) \quad (14)$$

The Franghiadakis/Tzanetakis[16] model follows the relation given by,

$$T_c = T_a + 0.031 * G - 0.058 \quad (15)$$

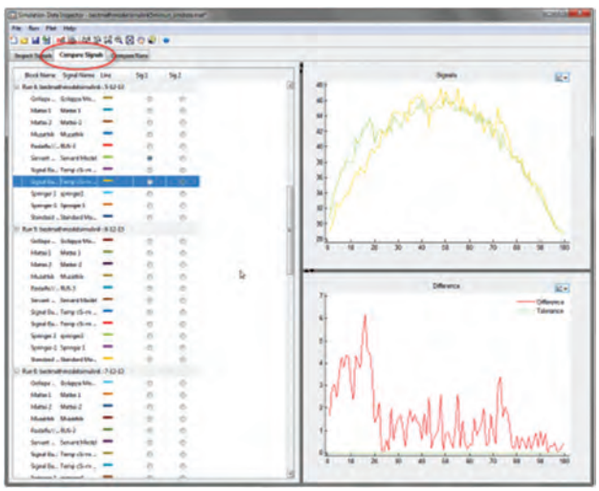

Fig. 6. Signal comparison with simulation data inspector.

It is observed daily average was not a good estimate of the model's accuracy in real time. As a result, few of the models are tested for data obtained every second and data averaged for every 5 minutes. Only a few models are considered because, the daily average gives an idea of well behaving models but does not accurately bring out how well they behave. Thus it would be fruitful to only test the accuracy of well behaving models.

Carrying out computation on data of such large volumes using MS-Excel in this case would be monotonous and time consuming. Therefore there arises a need to simplify this process and make it less intense. This is achieved linking the data with MATLAB and Simulink. With these tools it can be seen that the process of working with and visualizing data becomes simpler and more effective.

About two standard models as shown in Figure 5 are compared for their performance to the five minute averaged data and the data obtained every second. The behavior of the graphs obtained can also be compared with the graph expected. This allows to look in detail for the regions of time during which different models perform well as shown in Figure 6. This opens the possibility of combining various models for different periods of the day. In addition to this, inferences can be drawn by observing the graphs. Finally, results are obtained from which the need for an alternate modelling approach is considered.

4. TEMPERATURE PREDICTION WITH NEURAL NETWORKS

Artificial Neural Networks (ANN) have been considered as an alternate approach for prediction. ANNs are extremely useful in cases where the relationship between data is nonlinear and difficult to predict. However, the effectiveness

Table II. The scoring of architectures.

Network architecture	Training	Testing	Total
16×16	0.97106	0.97169	0.97116
$16 \times 16 \times 16$	0.97791	0.9774	0.97783
$10 \times 10 \times 10 \times 10$	0.97322	0.97282	0.97316
$10 \times 10 \times 10$	0.96389	0.96849	0.96841
10	0.94438	0.94392	0.94431

of an ANN increases if all the parameters affecting the system are known. From the observations of the previous sections, it is seen that the parameters affecting the cell temperature are wind speed, ambient temperature, irradiance and relative humidity.

In order to get a good generalization of the system under consideration, it is necessary to arrive at the most optimum architecture. However, there exist no fixed methods to accurately determine the number of neurons or number of hidden layers. An excess number of neurons tend to overfit the system and a number too less tends to underfit it. The hidden layers function to model the non-linearity of the system and each layer tries best to represent a feature of the system. It is a usual practice to determine the network architecture by trial and error.

In this paper, in order to determine the network architecture numerous runs with different number of neurons and hidden layers were tested. The measure of a networks performance is its MSE (Mean Squared error). The architectures with lowest mean square error were judged the best performing ones. The performances of the different architectures are explained below. All architectures were derived from the results of Bayesian regulation as the training algorithm is better than LevenbergMarquardt. In ANN, it is considered a general rule of thumb to select the number of neurons from 1 to 4 times the number of input parameters.

Table II shows the scoring of different architectures of neural networks run. From the table it can be seen that the $16 \times 16 \times 16$ network has the best score for the training and test dataset and thus the lowest MSE among all the models. For further tests the $16 \times 16 \times 16$ network, as shown in Figure 7, is selected to best represent the 12 day data. Figure 8 shows the scoring of this network.

5. RESULTS, OBSERVATIONS AND INFERENCES

Based on the values obtained a number of inferences are drawn to proceed towards the further stages. Among all the

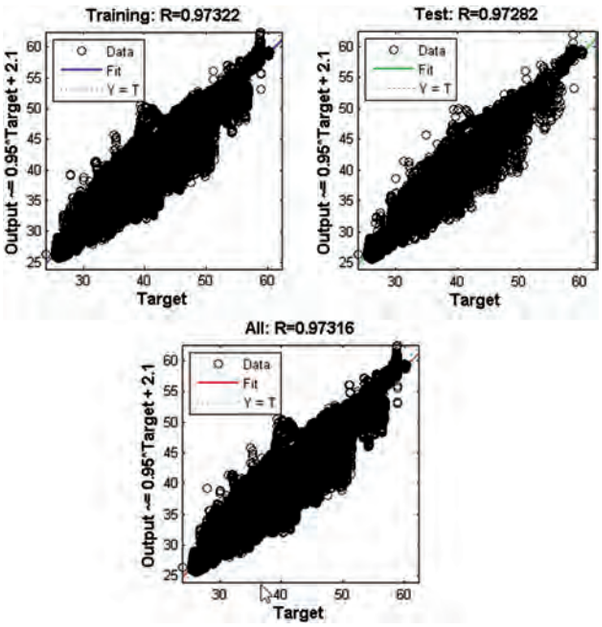

Fig. 8. Scoring of the network.

models obtained the ones with both lesser means and lesser standard deviations were considered well behaved models for this application. It necessary to have both values as low as possible since lower errors with higher standard deviations also signify unreliable models. Based on this criterion it could be seen that from Tables III and IV, the models which fell into the category of well-behaved were, the Servant model.

Further, the well behaved models were subjected to few samples of second by second data and evaluated. Upon doing so, it was seen that the models start deviating from their expected behavior. This deviation is characterized by a particular time in the day, namely when the irradiation is at high values or in other words, the peak hours of sunlight. In the off peak hours, the models are relatively well behaved and have less error. The inference drawn was that at peak hours the solar panel is heated to higher temperatures than off peak hours. As a result, by Newton's law of cooling we have,

$$\frac{dT(t)}{dt} = -r(T(t) - T_{\text{env}}) \tag{16}$$

From Eq. (16), it can be seen that hotter bodies cool faster than cooler bodies i.e., rate of heat loss is more for hotter bodies. Since at peak hours the solar panel behaves like a

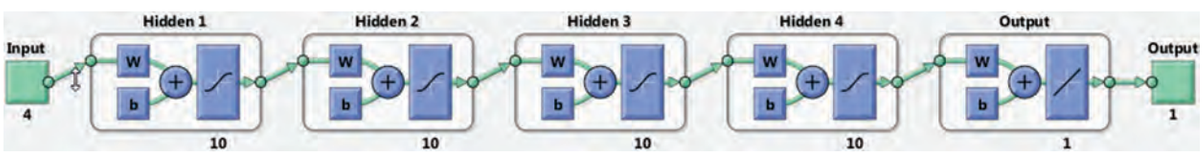

Fig. 7. A $10 \times 10 \times 10 \times 10$ network.

Table III. Performance of mathematical models for daily averages.

	C-Si PV module		CIS PV module	
	MAE%	Standard deviation	MAE%	Standard deviation
Ross thermal model (mast common model)	26.54	17.26	20.57	16.47
Kurtz model	17.87	9.10	18.34	6.86
Koehl model	11.67	6.15	9.75	3.23
Scoplaki 2 model	11.81	8.49	9.17	5.05
Mattei 1 model	5.71	4.71	6.05	2.909
Mattei 2 model	7.88	5.08	8.49	11.36
Homer model	19.08	17.83	19.70	21.42
Muzathik model	8.35	4.69	9.31	2.62

Table IV. Performance of mathematical models for daily averages.

	C-Si PV module		CIS PV module	
	MAE%	Standard deviation	MAE%	Standard deviation
Radalfo/Umberto/Salvatore-1 model	14.35	6.54	12.37	3.44
Rodalfo/Umberto/Salvatore-2 model	16.52	5.77	14.94	3.39
Rodalfo/Umberto/Salvatore-3 model	7.18	4.2	5.39	2.69
McAdams model	15.27	10.33	12.20	8.03
Servant model	2.98	4.122	2.42	2.818
King model	29.63	6.25	27.43	3.66
Franghiadakis/Tzanetakis model	18.94	4.61	16.97	3.66

hot body it cools faster than it would have at lower temperatures. As a result, the change in cell temperature is more rapid. Since the mathematical models have not accounted for heat flows these rapid changes are not accounted for in them. As a result, at higher temperatures the models deviate largely.

Table V. Performance of mathematical models for data sampled every second.

	Servant model		Bosch model	
Date	MAE (in °C)	Standard deviation (in °C)	MAE (in °C)	Standard deviation (in °C)
1/12/2013	2.81	2.93	4.67	3.83333
2/12/2013	3.255	2.479	5.138	2.476
3/12/2013	2.483	2.2625	5.625	3.3938
4/12/2013	2.89	2.392	4.533	3.037
5/12/2013	1.514	1.363	4.738	2.481
6/12/2013	1.797	1.206	4.347	2.428
7/12/2013	1.508	1.115	3.483	2.509
8/12/2013	2.719	2.197	4.0953	2.873
9/12/2013	3.142	1.922	2.195	1.577
10/12/2013	2.438	2.066	2.69	1.814
11/12/2013	2.232	1.329	2.282	1.699
12/12/2013	2.709	2.577	2.253	1.817
Average	2.426	1.986	3.837	2.495

Table VI. Performance of mathematical models for data averaged over 5 minutes.

	Servant model		Bosch model	
Date	MAE (in °C)	Standard deviation (in °C)	MAE (in °C)	Standard deviation (in °C)
1/12/2013	4.21	3.52	3.11	2.253
2/12/2013	2.559	3.089	2.767	2.132
4/12/2013	4.209	2.894	1.841	1.656
5/12/2013	2.514	2.192	1.927	1.396
6/12/2013	2.396	1.911	2.35	1.73
7/12/2013	1.506	0.9777	1.403	1.263
8/12/2013	2.376	1.865	2.596	2.11
9/12/2013	2.076	1.855	3.416	2.443
10/12/2013	2.1314	1.73	2.758	2.038
11/12/2013	1.838	1.194	2.401	1.842
12/12/2013	2.972	3.092	1.534	1.34
Average	2.617036	2.210882	2.373	1.836636

5.1. Validation with Simulink

Two standard models are considered for comparison, the Servant model and a model developed at Bosch. For the data obtained every second the Servant model gives lesser mean error and Standard Deviation. However for the 5 minute average data the Bosch model performs slightly better. This can be observed in Tables V and VI. From the graphs generated by the workflow, a noticeable trend is recorded. The fact that the deviation of the Servant model is more for the beginning of the day than the Bosch Model is seen. However after a particular point for all days, the Servant model starts behaving much better

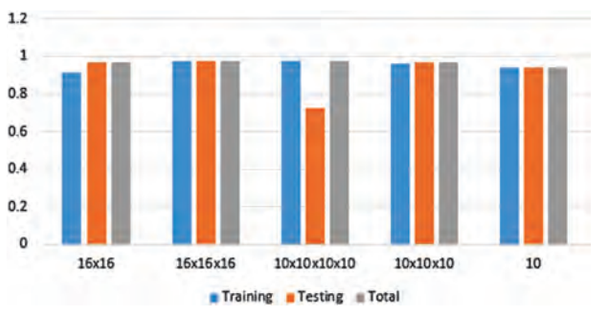

Fig. 9. The scoring of the architecture.

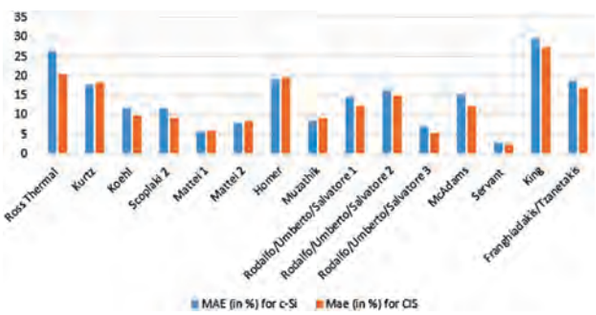

Fig. 10. The performance of different mathematical models.

RESEARCH ARTICLE

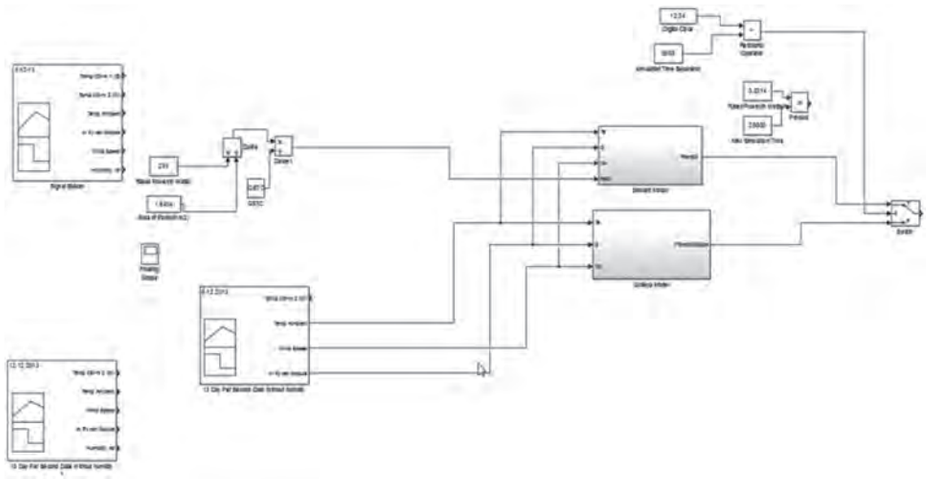

Fig. 11. The fused model.

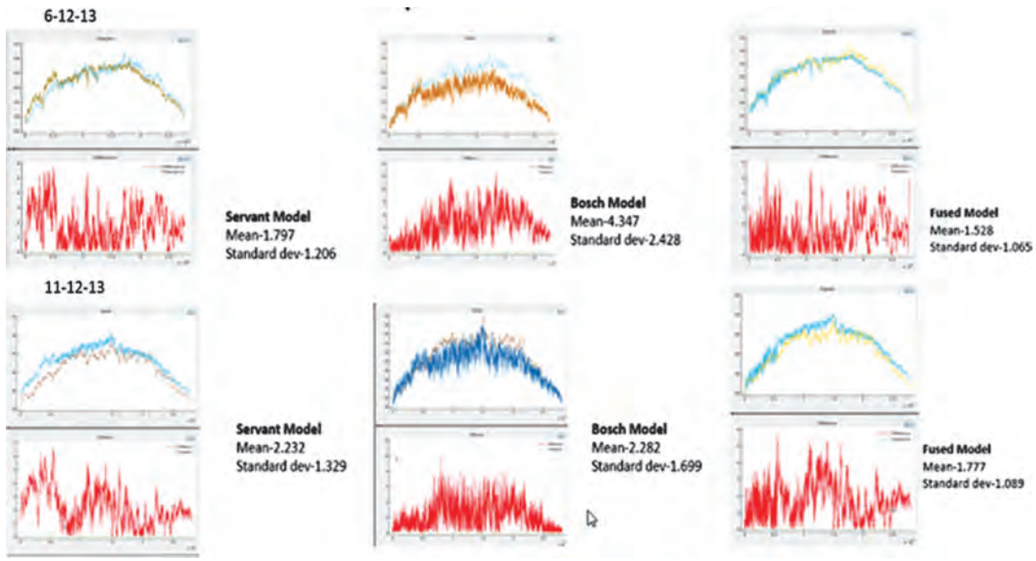

Fig. 12. Advantages of the fused mode.

than the Bosch Model. We thus observe that for two parts of the dataset, the models behave differently, with one model tracking one part of the data better than the other.

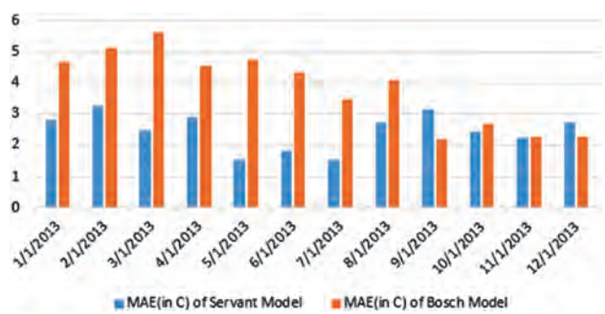

Fig. 13. Performance of mathematical models for data averaged over 5 minutes.

Table VII. Comparison of fused model with the ANN.

	Fused model		$16 \times 16 \times 16$ ANN	
Date	MAE (in °C)	Standard deviation (in °C)	MAE (in °C)	Standard deviation (in °C)
1/12/2013	2.662	2.78	0.9665	1.086
2/12/2013	3.341	2.382	1.12	1.238
3/12/2013	2.362	2.181	1.067	1.065
4/12/2013	2.909	2.416	1.204	1.173
5/12/2013	1.128	0.9085	0.7425	0.6408
6/12/2013	1.543	1.066	0.8607	0.7703
7/12/2013	1.472	1.142	0.7814	0.7629
8/12/2013	2.651	2.166	1.348	1.32
9/12/2013	2.424	1.474	0.9954	0.9869
10/12/2013	1.743	1.256	0.6127	0.5025
11/12/2013	1.772	1.084	0.6573	0.577
12/12/2013	2.339	2.418	0.9981	1.038
Average	2.153	1.772	0.944	0.930

RESEARCH ARTICLE

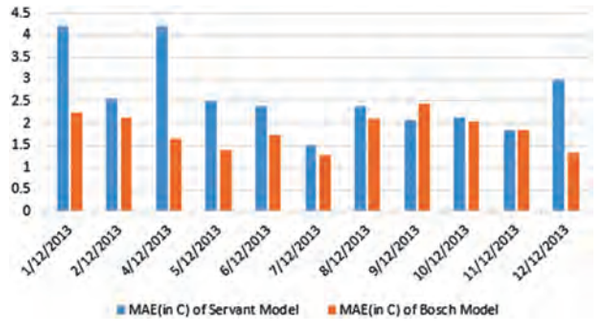

Fig. 14. Performance of mathematical models for data averaged over 5 minutes.

In order to increase the accuracy of the process, both the models were fused, as shown in Figure 9, to make sure that they operate in their favorable regions. The point of fusion was selected by visual inspection of the point after which the behavioral change was noticeable. The improvement in the fused model is shown in Figure 10.

The mathematical models in literature seldom considered humidity as a parameter affecting cell temperature. However, from the workflow, it was established that humidity was a parameter to be considered for temperature prediction as well, since. Figure 11 shows the error graph at high values of humidity. In Figure 12, it can be seen that at low values of relative humidity the error is less but at higher values the error starts increasing. This implies that there is a need to consider humidity as a parameter affecting cell temperature as well.

5.2. Results of Neural Networks

Figure 13 shows the ANN model versus the fused model in Simulink. It is observed that the neural network model performs better on all days of the dataset with an average error of only 0.944 degree which is only about 1.5–4% of the actual temperature, as shown in Table VII, since the cell temperature usually varies from 25–65 °C. This is much lower than the average error of 2.153° obtained in the fused model which is about 5–10% of the actual temperature.

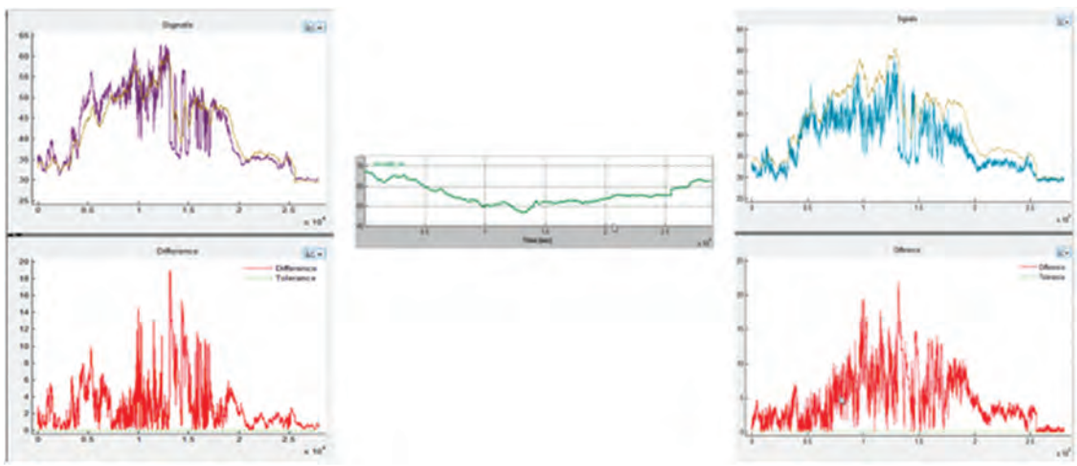

Fig. 15. Temperatures at high values of relative humidity. The *y*-axis represents the absolute temperature in the upper panes and the error in degrees in the lower panes. The *x*-axis represents the passage of time.

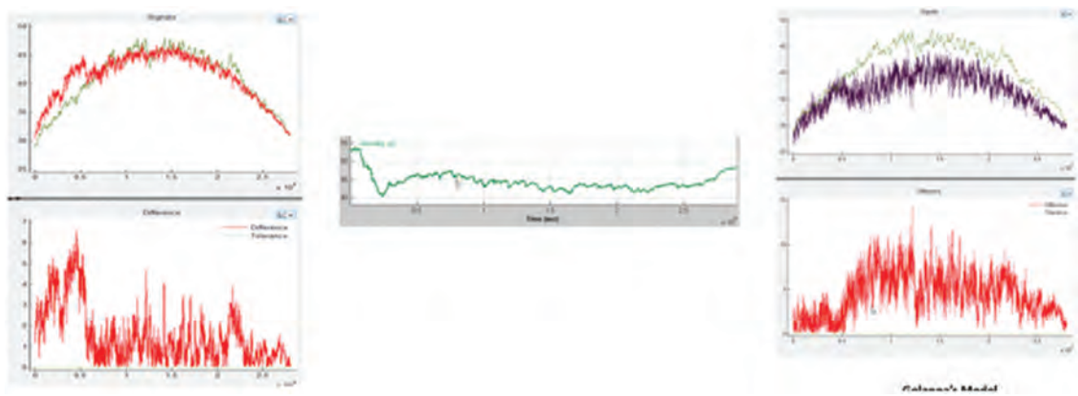

Fig. 16. Temperatures at low values of relative humidity.

RESEARCH ARTICLE

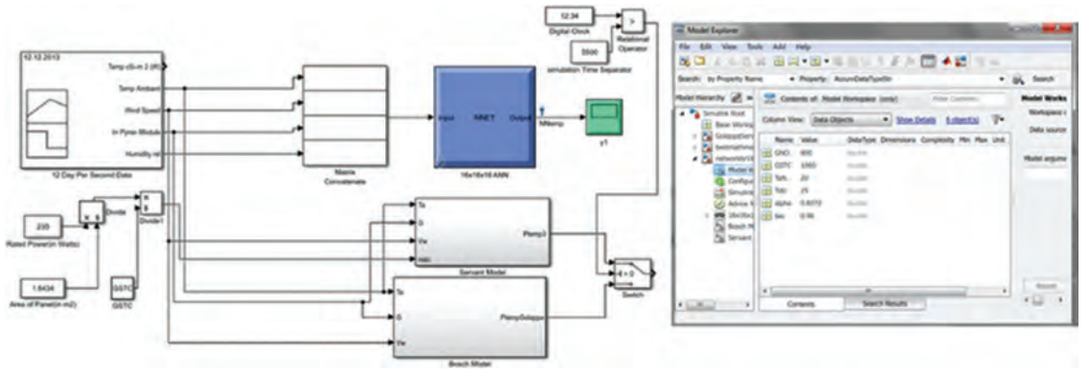

Fig. 17. The ANN versus the fused model.

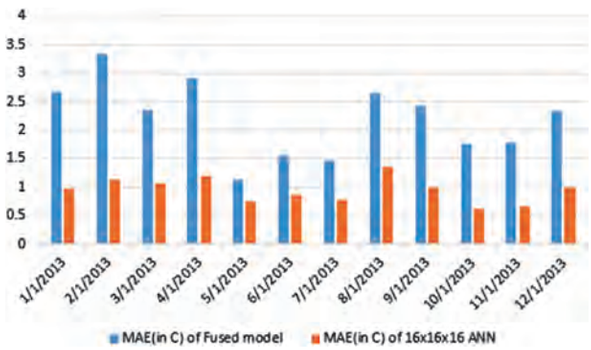

Fig. 18. Comparison of fused model with the ANN.

Even though the mathematical models were developed considering semiconductor physics, energy balance conditions and so on, there are many factors whose effects cannot be modelled properly because of their randomness or lack of understanding. One example can be the effect of the flow of hot air over a hot plate. Although a neural network does not explicitly solve these problems, their effects are inherently modelled into the network and can increase the accuracy of prediction.

6. CONCLUSION

An extensive study of existing mathematical models acclimatized to cooler regions by testing them for different solar panels was conducted. Few of the models were found to be generic and relatively relevant for tropical conditions. Moreover, a combination of existing models based on the time interval of interest proved to be more functional than the models standalone. In addition to this, models rarely consider humidity as a metric. This could possibly be attributed to effect of humidity being lower in the regions where the models were developed. However, in tropical countries, the effects of humidity cannot be ignored and should be taken into consideration. As a consequence, while developing a neural network, the relative humidity was also considered an important feature along with ambient temperature, irradiation and the wind speed. In the end a neural network which can predict temperature with an error of 3.5% to 5% is obtained.

In the future, the model developed in the paper can be made more versatile. This is achieved by testing and validating the same against more diverse data i.e., data spread over a various seasons. In addition to this, mathematical models involving humidity may also be further developed as their existence is very scarce. The cell temperature predictor can also be made more robust by modelling irradiance, wind speed and ambient temperature throughout the year. As a result of this, it possible to obtain a model which can predict the cell temperature by giving time and day of the year as inputs.

Acknowledgment: We are extremely grateful to the management of Robert Bosch Engineering and Business Solutions India Pvt. Ltd. for their support and guidance for this paper publication.

References

1. Available at: http://seci.gov.in/content/innerpage/intro-solar-park.php.
2. Ahmed Elnozahy, Ali K. Abdel Rahman, Ahmed Hamza H. Ali, Mazen Abdel-Salam, and S. Ookawara, *Energy and Building* 88, 100 **(2015)**.
3. R. Araneo, U. Grasselli, and S. Celozzi, *International Journal of Energy and Environmental Engineering* 5, 1 **(2014)**.
4. M. E. Ya'acob, H. Hizam, T. Khatib, M. Amran M. Radzi, C. Gomes, A. M. Bakri, M. H. Marhaban, and W. Elmenreich, *Journal of Renewable and Sustainable Energy* 6 **(2014)**.
5. A. Q. Jakhrani, A. K. Othman, A. R. H. Rigit, and S. R. Samo, *World Applied Sciences Journal 14 (Special Issue of Food and Environment)* 14, 01 **(2011)**.
6. G.-A. Migan, Study of the operating temperature of a PV module, Project Report, 2013 MVK160 Heat and Mass Transfer, May **(2013)**.
7. A. M. Muzathik, *International Journal of Energy Engineering* 4 **(2014)**.
8. K. Han, D. Shin, and Y. Choi, *International Journal of Emerging Technology and Advanced Engineering* 2 **(2012)**.
9. Bosch Solar Module c Si M 60 Datasheet, Available at: http://www.bosch-solarenergy.com/media/bosch_se_serviceorganisation/product/datenblaetter_2/kristtalin/au/Bosch_Solar_Module_c_Si_M_60_EU30117EU30123.
10. Bosch Solar Module CIS Datasheet, Available at: http://www.bosch-solarenergy.com/en/bosch_se_serviceorganisation/product/portfolio_2.html.

RESEARCH ARTICLE

11. E. Karatepe, M. Boztepe, and M. Colak, *Energy Conversion and Management* 47, 1159 **(2006)**.
12. A. A. H. El-Din, Ahmed H. H. Ali, and C. F.Gabra, Effect of ambient temperature on performance of different types of PV cells at different location in Egypt, *Middle East Power Conference (MEPCON'14)* Cairo, Egypt, December **(2014)**.
13. H. A. Rahman, K. M. Nor, M. Y. Hassan, S. Thanakodi, M. S. Majid, and F. Hussin, Modeling and simulation of grid connected photovoltaic system for Malaysian climate using matlab/simulink, *2010 IEEE International Conference on Power and Energy (PECon2010)*, Kuala Lumpur, Malaysia, November **(2010)**, pp. 935–940.
14. Schwingshackla, M. Petittaa, J. E. Wagnera, G. Belluardoc, D. Moserc, M. Castellia, M. Zebischa, and A. Tetzlaff, *Energy Procedia* 40, 77 **(2013)**.
15. G. Ciulla, V. Lo Brano, and E. Moreci, *International Journal of Photoenergy* 2013, Article ID 192854 **(2013)**.
16. Skoplaki and J. A. Palyvos, *Renewable Energy* 34, 23 **(2009)**.
17. F. Brihmat and S. Mekhtoub, PV cell temperature/PV power output, relationships homer methodology calculation, *IPCO-2014*, Bonn, Germany, June **(2014)**, ISSN 2356-5608.
18. Available at: http://www.pveducation.org/pvcdrom/solar-celloperation/effect-of-temperature.
19. P. Bacher, H. Madsen, and H. A. Nielsen, *Solar Energy* 83, 1772 **(2009)**.
20. M. K. Fuentes, A Simplified Thermal Model for Flat-Plate Photovoltaic Array, Technical report, Sandia National Laboratories, Albuquerque, New Mexico, May **(1987)**.

Received: xx Xxxx xxxx. Accepted: xx Xxxx xxxx.

RESEARCH ARTICLE